VELOCITY PROFILES FOR PARTICLES AND LIQUID IN OPEN-CHANNEL FLOW WITH SUSPENDED SEDIMENT

By M. Muste,[1] Associate Member, ASCE, and V. C. Patel,[2] Member, ASCE

ABSTRACT: Experiments were performed to measure the mean velocity and turbulence characteristics in open-channel flows with and without suspended sediment (alluvial sand of nearly uniform size). Velocity measurements were obtained by using a newly developed technique, the discriminator laser-doppler velocimeter (DLDV), which can distinguish both liquid and sediment particle velocities. The mean velocity of sediment particles was found to be lower than that of the water. While the velocity fluctuations in the water were not changed with the addition of sediment, those of the sediment were diminished. For the range of concentrations considered, the friction velocity and the free-surface slope increased with sediment concentration unlike other bulk flow parameters, which were practically constant. A uniform method of analysis was developed to facilitate data interpretation and comparison between similar studies.

INTRODUCTION

In open-channel flows with suspended sediment, accurate information on particle and liquid velocities is crucial not only to understand fluid-particle interaction, but also for estimation of sediment transport rates and friction factor. The lack of a theoretical basis for predicting sediment behavior has meant that experiments play a critical role in the understanding of the underlying flow phenomena. However, difficulties of instrumentation, clear delineation of experimental conditions, and differences in techniques of data analysis have led to fragmentary and often contradictory experimental evidence. For example, use of pressure probes and hot films for measurement of velocity involves unknown sediment-probe interactions and measurement errors with no differentiation between liquid and particle velocities.

With the advent of optical and acoustic Doppler velocimetry, nonintrusive methods have been favored for velocity measurements in sediment-laden flows (Müller 1973; Van Ingen 1981; Tsuji and Morikawa 1982; Lyn 1988; Rogers and Eaton 1989; Song et al. 1994). Despite the improved accuracy of Doppler techniques compared to conventional ones, the difficulty of such systems to distinguish precisely between the signals arising from suspended sediment and those originating from seed particles following the liquid has impeded a full description of the velocity field in flows with suspended sediment.

The increased popularity of optical methods for measurements in multiphase flows led to extensions of laser-Doppler velocimetry (LDV), phase-Doppler anemometry (PDA), and more recently, particle image velocimetry (PIV), targeting flow-field diagnostics including velocity measurements in the carrier fluid along with velocity, concentration, and particle size measurements of the suspended fraction. Along this line, Parthasarathy and Muste (1994) and Muste et al. (1995) developed the discriminator LDV (DLDV), which combines a conventional LDV with an auxiliary optoelectronic unit for particle-size discrimination.

This paper describes the use of the DLDV system to separately measure, for the first time, sediment and liquid velocities in open-channel flows with transport of natural sand (i.e., irregular shaped particles). The data provide new insights on the flow field and, for the flow conditions selected for these initial tests, show that the velocity of sand particles is smaller than that of the water by as much as 4%. The implication of this result on the friction factor and on the von Karman constant in the velocity profile are discussed.

EXPERIMENTAL CONSIDERATIONS

Instrumentation

The experiments were performed in the Iowa Institute of Hydraulic Research (IIHR) sediment flume. This is a 30-m-long, 0.91-m-wide, and 0.45-m-deep glass-sided flume with a concrete bed. The water was recirculated by two 7.5-horsepower, variable-speed pumps via two 0.25-m-diameter return pipes. Orifice meters in these pipes were used to measure discharge with a resolution of 5×10^{-5} m^3/s. Damping of large-scale turbulence and secondary currents was achieved by means of a honeycomb at the flume entrance.

The flume was supported by a central pivot and four synchronized motor-driven jacks so that the bed slope could be adjusted without interrupting the flow. The slope of the bed could be measured by means of a point gauge, with an accuracy of 0.3 mm, at the downstream end of the flume. The slope of the water surface was measured using eight piezometers, spaced at 3.048-m intervals, fitted to the invert of the flume and connected to a bank of glass manometer tubes. A vernier with a resolution of 0.3 mm was used to measure the piezometer levels. Linear regression of the piezometer readings yielded an average water surface slope for which the propagated uncertainty was estimated to be 2.5%.

The test section was located 19 m from the channel entrance. Water surface elevations at this section were obtained using a point gauge mounted on the instrument carriage referenced to the same zero value. A digital thermometer located in the test section was used to measure the water temperature. To ensure temperature stability (the tap water was at 6°–8°C while the ambient temperature was 18°–20°C) the flume was filled 10–12 hours before starting the experiments.

Local mean sediment concentration was measured with a point sediment sampler similar to that used by Lyn (1986). The dimensions of the tip were selected such that both reasonable space resolution and good entrance conditions for the sand size investigated were obtained. The sampler was mounted on the instrument carriage at the same elevation as the DLDV measurement volume. Calibrations were performed prior to the experiments to establish the settings for withdrawing isokinetic samples of the sediment-water mixture.

The present investigation was designed to obtain a suspension of uniform sediment without deposition on the bed.

[1]Res. Assoc., Iowa Inst. of Hydr. Res., The Univ. of Iowa, Iowa City, IA 52242-1585.

[2]Dir., Iowa Inst. of Hydr. Res., The Univ. of Iowa, Iowa City, IA.

Note. Discussion open until February 1, 1998. To extend the closing date one month, a written request must be filed with the ASCE Manager of Journals. The manuscript for this paper was submitted for review and possible publication on November 6, 1995. This paper is part of the *Journal of Hydraulic Engineering*, Vol. 123, No. 9, September, 1997. ISSN 0733-9429/97/0009-0742–0751/$4.00 + $.50 per page. Paper No. 11976.

Therefore, the type of sand feeding system was of less importance [see also Jobson and Sayre (1970) and Parker and Wilcock (1993)]. For the recirculating system employed, a sand feed system consisting of a rotating sieve was used to quickly establish a stable concentration profile. The rotating sieve provided uniform feeding across the width of the flume forming a time-continuous line source of sand on the free surface.

The sediment used in the experiments had to comply with certain optical (homogeneous material) and size requirements (narrow size range, and compatible with the feeding system and the transport capacity of the flume). The best choice to fulfill these requirements were the sand deposits from the 1993 midwest flood on the banks of the Iowa River in the neighborhood of IIHR. This sand, in the size range of 0.044–0.710 mm, with D_{50} = 0.250 mm and a specific gravity of 2.65, was deposited from suspension during the flood. To further simplify the interpretation of the experimental results, uniform sediment size was employed; consequently, careful downsizing in the 0.21–0.25 mm size interval (ratio of consecutive sieve sizes given by the fourth root of 2 according to the Tyler standard) was performed.

The DLDV was employed for particle and liquid velocity measurements in clear-water and sediment-laden flows. The DLDV combines a conventional LDV system with an auxiliary discriminator system to distinguish signals originating from the fluid tracers from those arising from the sand particles. The discrimination procedure is performed optically and is completely independent of the LDV system. In the configuration employed, the LDV system was a conventional two-component, He-Ne laser based system whose main specifications are presented in Table 1. The discriminator consists of an additional photomultiplier aligned with the photomultipliers of the LDV receiving optics. Validation of the capabilities of the DLDV technique along with a detailed description of the underlying principle, electronic and optical arrangements, operation mode, and the expected accuracy of the measured data can be found in Muste et al. (1996).

TABLE 1. Specifications of Major Components of LDV System

Component (1)	Element (2)	Specifications (3)
Laser and transmitting optics	Laser: wavelength	632.8 nm (red)
	beam diameter $D_{e^{-2}}$	1.10 mm
	power	15 mW
	Beam separation	50 mm
	Beam half angle, φ	1.68°
	Dual beam to on-axis angle	±45°
Measurement volume	Fringe spacing d_f	10.75 μm
	Number of fringes	35
	Diameter d_m	0.38 mm
	Length l_m	9.00 mm
LDV receiving optics	Polarization separator	TSI 9142
	Photomultiplier	TSI 9162
	PMT power supply	TSI 9165
	Detection region: diameter	0.75 mm
	length	3.00 mm
Frequency shifter	Bragg cell	TSI 9180
Signal processor	Counter type	TSI IFA 550

Experimental Procedures and Flow Conditions

The present work was focused on open-channel flows with only suspended load, that is, no accumulation of sediment on the bed, as in the experiments of Coleman (1981). Similar flows were investigated in previous studies by Vanoni (1946), Jobson and Sayre (1970), Coleman (1981), Lyn (1986), Wang and Qian (1992), and Kereselidze and Kutavaia (1995).

Available facilities in the IIHR laboratory and the special requirements of sediment-laden flows and the DLDV system imposed limitations on the experimental conditions. Factors such as the flume aspect ratio, LDV data rate, sediment size range and concentrations, and modifications in bed roughness due to the presence of sediment, were all carefully considered and the final set of experimental conditions was a compromise among these requirements.

The experiments with sediment were conducted in three series, labeled SL01, SL02, and SL03, with concentration increasing in that order. To facilitate interpretation of the results, only a single parameter was varied, namely, the sediment concentration, keeping all others constant. Without sediment deposition anywhere in the flume, any change in the flow pattern after sand addition could be attributed only to the presence of suspended sediment. The saturation transport capacity was identified as that concentration for which ripples began to form on the channel bed. This condition was avoided in the experiments. As may be seen in Table 2, perceptible changes in the free surface slope occurred each time sediment was added, so that the three flows were clearly distinct and a basis of comparison among them had to be established. The major question was whether local parameters such as shear velocity (determined from near-bed velocity measurements) or bulk parameters of the flow such as depth or energy slope could be used as equivalence criteria. In the present work, a new approach was used for comparison: "equivalent" flows were defined as flows with the same energy input (slope). Consequently, the comparison was made between three pairs of sediment-laden and clear-water flows, each pair with the same free surface slope.

TABLE 2. Flow Parameters for Clear-Water and Sediment-Laden Flows

Parameter (1)	Units (2)	Clear-Water Flows			Sediment-Laden Flows		
		CW01 (3)	CW02 (4)	CW03 (5)	SL01 (6)	SL02 (7)	SL03 (8)
Discharge Q ($\times 10^{-3}$)	m^3/s	73.8	73.5	73.3	73.8	73.8	73.8
Depth h	m	0.130	0.128	0.127	0.129	0.129	0.128
Bed slope S_b ($\times 10^{-4}$)	—	7.39	7.68	8.13	7.39	7.39	8.13
Energy slope S ($\times 10^{-4}$)	—	7.41	7.71	8.11	7.42	7.68	7.97
Aspect ratio b/h	—	7.00	7.11	7.16	7.05	7.05	7.11
Hydraulic radius R	m	0.101	0.100	0.099	0.100	0.100	0.100
Mean bulk velocity U_m	m/s	0.624	0.628	0.634	0.629	0.629	0.633
Temperature T	°C	18.4	17.2	17.4	19.4	18.7	18.3
$R = 4U_mR/\nu$ ($\times 10^5$)	—	2.40	2.32	2.32	2.46	2.44	2.41
$F = U_m/\sqrt{gh}$	—	0.55	0.56	0.57	0.56	0.56	0.56
u_{*_1} = from Reynolds stress	cm/s	2.922	2.916	2.976	3.023	3.051	3.130
u_{*_2} = from log law	cm/s	3.044	3.110	3.100	3.238	3.251	3.268
$u_{*_3} = \sqrt{gRS}$	cm/s	2.710	2.753	2.810	2.701	2.745	2.796
$u_{*_4} = \sqrt{ghS}$	cm/s	3.074	3.112	3.178	3.064	3.117	3.164

Clear-water flows were studied not only to provide a basis of comparison with sediment-laden flows but also to verify the performance of DLDV under standard conditions. These experiments were also conducted in three series, labeled CW01, CW02, CW03, characterized by the parameters shown in Table 2. CW01 is the initial flow, while CW02 and CW03 are clear-water flows with the same free surface slope as the sediment-laden flows SL02 and SL03, respectively.

Starting with an initial clear-water flow, sediment was added gradually in three steps: 0.5 kg, 0.5 kg, and 1.0 kg. The addition of sediment was slow compared to the recirculation time for the flow in the flume. After every addition, a recirculation time was allowed, followed by bed slope adjustments to attain the uniform flow. No other parameter was changed on purpose. During the measurements, the flume was regularly inspected to ensure that no sand was deposited anywhere. Despite the long duration of the experimental runs, good spatial and temporal stability of sediment lines in the near-bed region was observed leading to the conclusion that the mean sediment concentration remained constant throughout the experiments.

Using the point gauge at the downstream end of the flume for the bed slope and piezometers for the free-surface slope, the two slopes were monitored. For the sediment-laden flows, the uniformity of the flow was achieved by repeated adjustments of the bed slope until it matched the free-surface slope. For the clear-water (reference) flows, the target slope for the bed was set and the depth was adjusted until the free-surface slope equaled the bed slope. The maximum nonuniformity (the difference between energy and bed slopes) of sediment-laden flows did not exceed 4% (SL02 run) and 0.5% for clear-water flows (see Table 2).

High-flow velocities required by sediment suspension considerations combined with the small depths used resulted in fluctuations of the free surface, with amplitudes estimated at ± 3 mm. The use of piezometers completely smoothed the effect of the free-surface waves in the determination of the free-surface slope. The stability of the piezometer readings during the measurements suggested the greater reliability of this method for depth measurements over point gauges. The piezometer positioned in the test section, and calibrated against precise depth measurements with still water, was used for measurement of flow depth.

For concentration measurements, 1-liter bottles were used for sampling, maintaining a constant head during the filling. After sediment had settled, the samples were filtered, oven-dried and weighed on an electronic balance. The measured volumetric concentrations at $y/h = 0.15$ (the first near-bed location of the DLDV measurement) were 3.77×10^{-5} (100 mg/l) and 6.53×10^{-5} (173 mg/l) for SL02 and SL03 sediment-laden flows. The sand collected for the SL01 flow was too small to accurately determine the concentration.

In all the flow conditions investigated, care was taken to ensure fully developed conditions as well as stability and repeatability of the flows. All measurements for each flow were taken in one run in order to avoid variations of parameters that were otherwise difficult to control, for example, ambient temperature and water cleanliness. The duration of the run varied between 6 and 15 hours. Repeated measurements (at least three times for each experiment) of flow parameters such as free-surface slope, temperature, depth, and discharge, were within experimental uncertainties. When measurements were made in sediment-laden flows, the procedures included checks for repeatability of the previous measurements. To avoid signal attenuation on the DLDV photomultipliers (PMTs), the water in the flume was replaced and the added sediment was prewashed.

Weak secondary currents were undoubtedly present in the experiments in spite of the large aspect ratios employed. This was inferred from three distinct sand strips in the near-bed region containing several lines of sediment particles. These strips appeared after the first sediment addition, (SL01 flow) and were located symmetrically with respect to the walls. As the concentration was increased, the number and widths of the strips increased (to six strips), coalescing at higher concentrations into a continuous layer of sand moving along the bed. In the three experiments for which data are presented here the latter configuration was not present.

Fully developed flow conditions and the level of secondary currents in this flume were documented in earlier experiments by Parthasarathy and Muste (1994). Based on these findings and the high aspect ratios (not less than 7), it was concluded that the present flows were fully developed, with secondary flows having a negligible effect on the measurements in the channel center plane.

DLDV Operation

For velocity measurements in clear-water and sediment-laden flows the DLDV was set in forward 5° off-axis configuration, as shown in Fig. 1. The DLDV settings were as follows:

- High gains on LDV PMTs, even time (ET) collection mode for clear-water flows and for liquid in sediment-laden flows.
- Low gains on LDV PMTs, time between data (TBD) collection mode for particles in sediment-laden flows.

High or low gains on the PMTs were used alternatively in order to enhance the contributions of either particles or liquid in the velocity files depending on what was intended to be measured. The LDV processors, IFA 550 (TSI Inc.) employed signal correlation to reject noise, with an output compatible with counter-type processors. By choosing the ET collection mode on the signal processors, the real time history of the flow is distorted compared to the TBD mode. This did not pose any restriction of the present results because spectral analysis was not considered. The liquid velocities in sediment-laden flows were obtained by splitting the files recorded with high gains on PMTs; according to a set discrimination criterion, velocities were associated either to fluid or sediment particles. The same procedure was used to separate particle velocities from the files recorded with low gains on PMTs.

Prior to making measurements with DLDV, an evaluation of the turbulence scales was necessary. Table 3 contains the relevant temporal and spatial scales estimated from preliminary measurements. This information, along with the LDV characteristics summarized in Table 1, provides estimates of the appropriateness of the temporal and spatial resolution of the measurement method.

The temporal resolution of DLDV involves, in addition to the frequency response of the electronic components, the type of signal processing employed. However, given the fact that only averaged values were of interest, the sampling frequency of the signal processors was less important. In contrast, the total collection (averaging) time required special consideration for both first- and higher-order moments. When the ET mode

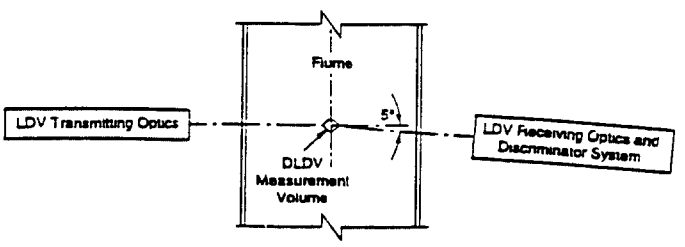

FIG. 1. Optical Arrangement for Liquid and Particle Velocity Measurements

TABLE 3. Turbulence Length and Time Scales (Selected)

Parameter (1)	Value (2)
Outer length scale h	129,000 μm
Viscous length scale ν/u_*	35 μm
Kolmogorov length scale[a] $\ell \cdot (R_T)^{-3/4}$	135 μm
Outer time scale h/U_m	205 ms
Viscous time scale ν/u_*^2	1 ms
Kolmogorov time scale[a] $\ell \cdot (R_T)^{-1/2}/u$	17 ms

[a] $R_T = u\ell/\nu$; $u = \sqrt{q^2} = \sqrt{u'^2_{RMS} + v'^2_{RMS} + w'^2_{RMS}}$; $\ell \sim h$; $w'_{RMS} = 1/2(u'_{RMS} + v'_{RMS})$; evaluation at the first near-bed location.

(coupled with high gains on the LDV PMTs) was used for data acquisition, the data rate was larger than 1,000 Hz throughout the depth; therefore, a collection time of 500 s with a sampling time of 20 ms was found satisfactory. The selected sampling time was correlated to the average transition time of sand particles to ensure that only one measurement per particle was made. The liquid velocities recorded in this mode contained approximately 20,000 data points per file.

When the TBD acquisition mode was used, implying low gains on the LDV PMTs, the data rate dropped to as low as 10–12 Hz. In this case each data point represents measurement on one particle (and, given the frequency value, obviously no repeated measurements for the same particle) and the question of averaging had to be addressed in terms of how many particles were necessary for meaningful statistics of the sample. Limited by the total time of an experiment, and taking into account similar experiments (Parthasarathy 1989), the samples for particle velocities contained at least 200 data points obtained from two measurements for each location. Because of this limitation, the $-\overline{u'v'}$ correlation for the particle velocities is not reliable. In any case, the physical significance of such a correlation for particles is also not clear.

The size of the recorded files (required by the software associated with the signal processor prior to data acquisition) was selected such that a collection time of 500 s was needed in all measurements performed; therefore, both ET and TBD collection modes used the same time for data collection. The coincidence window width of 1 ms was correlated with the average transit time for the largest particles in the flow so as to assure that the velocity measurements were made on the same particle.

For each experiment, measurements of each type of velocity file were taken and analyzed, and then discarded, prior to obtaining the final record in order to control the DLDV settings. During the tests, data processing parameters (threshold selection), its output (stability of the statistics), the level of beam extinction and its effect on the threshold selection, the cross-talk between LDV channels, and signal coincidence for the LDV and discriminator were all verified.

For each flow condition, velocity measurements at 18 non-equally spaced locations across the depth in the center plane of the flume were taken using the DLDV: the first seven near the bed were 3 mm apart, followed by five in 6-mm steps, with the last five measurements at 9-mm intervals. To satisfy the signal validation criterion of the LDV system, a 45° orientation of the two pairs of laser beams with respect to the dominant flow velocity component was employed. This requirement precluded measurements closer to the bed or the free surface. The liquid velocity measurements at the first three near-bed locations, and the particle velocity measurements at all locations were repeated.

Uncertainty analysis for the DLDV system was presented elsewhere (Muste 1996) hence, it is only briefly presented here. Directional ambiguity and bias were eliminated by employing a frequency shift of 100 kHz. Fringe bias was also eliminated by the use of this frequency shifting. In the ET mode, by sampling the velocity output at equal intervals of time larger than the average transition time of liquid tracers through the measurement volume, the velocity bias is also removed (Durst et al. 1981). This procedure is wasteful of signal output but is simple to implement. In TBD mode the statistics were computed only using the portions of the signal when the particles are in the measurement volume such that the velocity bias is eliminated.

The overall uncertainty (including bias and precision errors), computed according to the methodology that Figliola and Beasley used in 1991, gave the following uncertainty estimates: 4% of mean streamwise velocity for clear water, and 4% and 5% for water and particles in sediment-laden flows; 11% of streamwise velocity fluctuations for clear water, and 7% for water and 17% for particles in sediment-laden flows. For the vertical velocity component, the precision uncertainties were high due to the near-zero value of these velocities throughout the depth, and therefore, are not meaningful.

The rather large values of the computed uncertainties raises the question whether the instrumentation or the flow process are responsible for them. It should be noted here that the performance of the DLDV was tested through several preliminary tests where the effects of change of the gains on the PMTs, direction of detection, and particle properties were documented (Muste et al. 1996). The results were in agreement with the experimental evidence obtained previously in similar flow conditions. Such an example is an experiment in a small-scale sediment-laden jet (Muste 1995) where the shift in the axial velocity between the sediment and the underlying water jet varied between 11% and 88%. These differences are far beyond the typical LDV errors.

PRESENTATION OF RESULTS

Measurements

Dimensional velocity profiles are considered first because they do not involve parameter estimation such as the friction

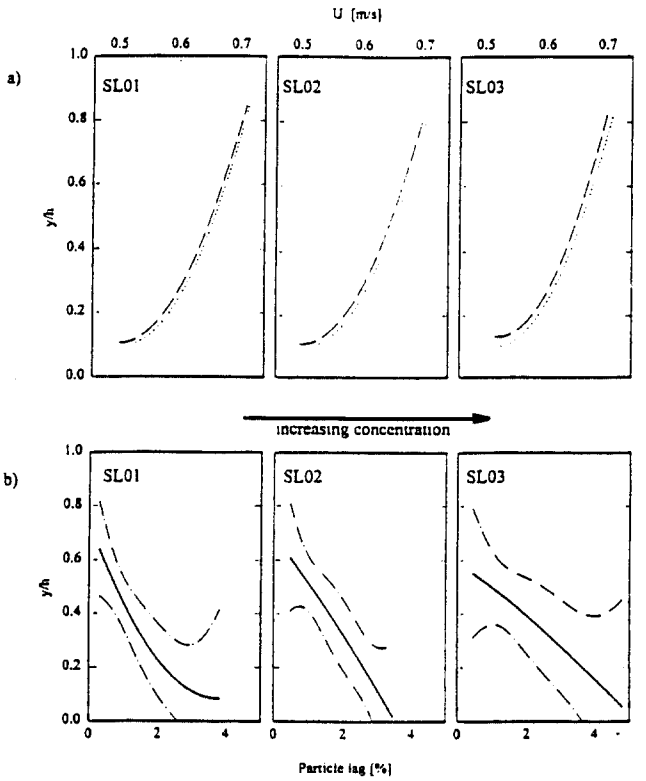

FIG. 2. Mean Velocity Profiles for SL01, SL02, and SL03: (a) Profiles for Liquid (Dotted Line) and Sediment (Dashed Line); (b) Difference between Profiles (Dash-Dotted Lines Indicate 95% Confidence Interval)

velocity and capture the essential physics of the flow. Profiles of mean velocities for both sediment particles and water in the three experiments, SL01, SL02, and SL03, are shown in Fig. 2(a). U is the mean streamwise velocity, y is the distance from the bed, and h is the flow depth. The measured data were smoothed to remove the scatter and to show an important result. Both the raw data for the velocity profiles as well as the regression lines fitted to them, as shown in Fig. 2(a), clearly indicate that, all across the depth, the particle velocity lags the liquid velocity, and the lag depends on concentration. The lag is not constant across the depth but increases near the bed. Similar observations were made by Summer and Deigaard (1981), Rashidi et al. (1990), and Wang and Ni (1991) in experiments using spherical particles with specific gravity in the range of 1–1.6. Based on this experimental evidence Aziz (1996) evaluated the errors involved when the relative velocity between sediment particles and fluid is considered.

The trends of the particle lag are more clearly illustrated in Fig. 2(b) where the particle lag, defined as the percentage difference between the liquid and particle velocity in the same flow, is shown. With increased sediment concentration, the particle lag is increased near the bed, but remains roughly the same in the upper region of the flow. A nondimensional plot U/U_{max} versus y/h may be more useful in identifying this feature but, as noted earlier, the measurements could not be carried out close to the free surface due to the nature of the LDV-beams configuration.

In the literature, the effect of sediment on the underlying flow is usually documented by comparison between the initial clear-water flow and the subsequent sediment-laden flows obtained by gradually adding the sediment. As pointed out earlier, present experimental evidence suggested the need for another approach to define an "equivalent" or "reference" flow. Here, comparisons are made in both ways to illustrate the differences, and particularly to reveal the underlying physics.

The plots in Fig. 3 show the measurements in the sediment-laden flows SL01, SL02, and SL03, each paired with the clear-water flow with the same energy slope, namely, CW01, CW02, and CW03. The data density, closeness of the velocity magnitude for all cases and the unavoidable experimental scatter make it difficult to obtain a clear picture of the flow changes from the actual measurements. Therefore, regression lines through the data (a linear regression to a second-order polynomial), instead of the actual measurements, are plotted. For the first pair, that is, SL01-CW01, it can be observed that the addition of very small quantities of sand, which are concentrated mostly near the bed, produces a shift of the water velocity profile that exceeds the initial clear-water profile. The observed pattern in the velocity shift is not unusual. Similar trends are observed in turbulent flows with small concentrations of polymeric filamentous additives. There is a vast amount of experimental evidence showing that in the absence of depositions at the wall, the addition of minute concentrations of polymer particles produces an increase of the mean bulk velocity and an interrelated friction reduction [for instance, Hoyt (1991)]. This positive effect is lost, however, when some optimum concentration of polymer is exceeded, beyond which the reverse effect (i.e., increase of friction) is observed. Similarly, in the present experiments, continuing the addition of sediment leads to a decrease in the water velocity all across the depth. Also, increase in sand concentration leads to a larger reduction in water velocity.

It should be emphasized that the trends described here were distinguished only after introducing the aforementioned definition of equivalent flows. Initially, when the SL01, SL02, and SL03 data were compared with only CW01 as reference flow (the conventional approach), as illustrated in Fig. 4, the trends would have led to a different conclusion, namely, that the liquid velocity in sediment-laden flow is increased continuously with sediment addition, a fact that contradicts energy balance considerations.

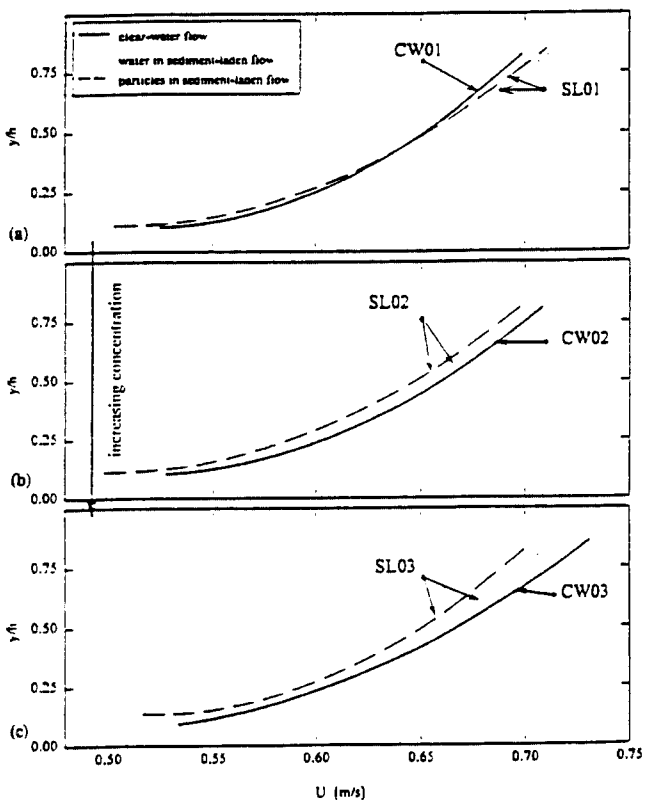

FIG. 3. Comparison of Mean Streamwise Velocity Profiles for Clear-Water, and Sediment and Water in Sediment-Laden Flows (Same Energy Slope); Regression Lines

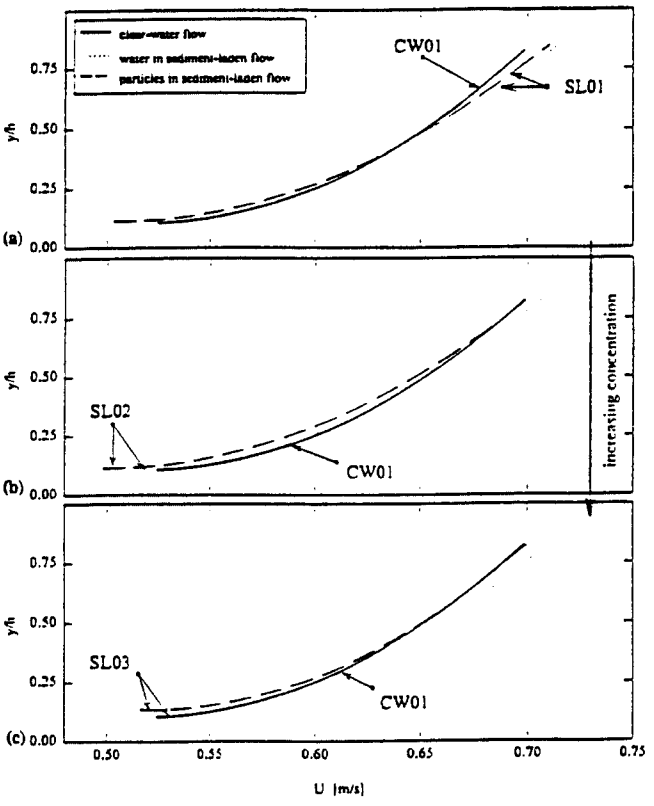

FIG. 4. Conventional Comparison of Mean Streamwise Velocity Profiles in Clear-Water and Sediment-Laden Flows; Regression Lines

Data Analysis

In any experimental study conducted under similar conditions, the scatter in the results and/or conflicting conclusions may be attributed to differences in instrumentation and experimental conditions, as well as to different methods of data analysis. For example, it is known that the logarithmic plot, which is extensively used for graphical representation of the mean velocity, is highly sensitive to small variations (±5%) of its parameters and, depending on the procedure adopted for curve fitting, the values obtained for the derived quantities may vary significantly (Coleman 1981). This fact is in conflict with the generally accepted idea in the literature that ±5% variation in any of the measured parameter is within the limits of experimental uncertainties. Moreover, as Valiani (1991) and Yalin (1977) pointed out, analysis of few selected flows from an experimental investigation (based on some of the reference parameters) may lead to different conclusions from those inferred from the investigation as a whole. Therefore, it is not surprising that similar experimental studies, using different techniques for data analysis, can lead to quite different interpretations of the physical processes involved.

As the friction velocity, u_*, which is used in the analysis of the velocity profiles, is the quantity most likely to be subjected to errors from both experimental methods and data analysis, in the present work its evaluation was made using four methods as follows.

1. Assuming a linear variation of the total (molecular plus turbulent) shear stress τ, from τ_b, the value at the bed ($y = 0$), to zero at the free surface ($y = h$)

$$\frac{\tau}{\rho} = -\overline{u'v'} + \nu \frac{\partial U}{\partial y} = u_*^2 \left(1 - \frac{y}{h}\right) \tag{1}$$

   where u_* was determined by extrapolation of the measured distribution of the Reynolds stress $-\overline{u'v'}$ to the wall, the contribution of the molecular stress being negligible.
2. u_* was obtained using the method of Clauser, in which the measured mean velocity profile $U(y)$ in the wall region ($y/h < 0.2$) was fitted to the log law

$$u^+ = \frac{1}{\kappa} \ln y^+ + B \tag{2}$$

   where $u^+ = U/u_*$; $y^+ = u_* y/\nu$; κ = von Karman coefficient; and B = constant that depends on bed roughness.
3. From momentum balance, u_* is related to the channel slope S and the hydraulic radius R by

$$u_* = \sqrt{gRS} \tag{3}$$

   As the shear velocity varies around the perimeter, this gives an average value of u_*.
4. For a two-dimensional fully developed flow, or flow in a wide channel (aspect ratio greater than about 6), the depth h is used in place of the hydraulic radius, and

$$u_* = \sqrt{ghS} \tag{4}$$

For the present experiments, where the agreement with the linear variation of the Reynolds stress was good for all flows, method 1 was considered the most reliable; nevertheless, method 2 requires 10–12 mean-velocity measurements in the near-bed region for a reliable curve fit whereas in the present experiments only six were available. In general, methods 3 and 4 were of less accuracy because they incorporate errors due to piezometers and flow depth readings. Moreover, differences in bed and side-wall roughness characteristics must be accounted for in method 3; due to difficulties in the quantification of the roughness characteristics, these differences were not taken into consideration here. Also, it was assumed that the high aspect ratio removes the effects of sidewalls. No correction for the kinematic viscosity [as proposed by Coleman (1981)] was considered because of the small sediment concentrations involved. Even for larger concentrations, as in Coleman's experiments, the variation in the viscosity of the mixture was negligible.

In a two-dimensional turbulent flow of a homogeneous fluid the basic assumptions and dimensional analysis that lead to similarity of the near-wall flow, implying a constant value of κ, also lead to universal correlations for the turbulent fluctuations (Nezu and Rodi 1986). $\kappa = 0.412$, proposed by Nezu and Rodi (1986), and reconfirmed by recent studies (Prinos and Zeris 1995), was used in the present work. Experimental results in sediment-laden flows due to Coleman (1981), theoretical arguments presented by Lyn (1988), and perhaps more important the need for a uniform method for data analysis for these types of flows, all led to the assumption that κ remains unchanged in sediment-laden flows involving only suspended sediment and small sediment concentrations. With this value, the best fit of (2) to the experimental data provided u_* and the constant B.

Using an approach identical with that of Nezu and Rodi (1986), the friction velocity obtained by method 1 was used for nondimensional representation of the Reynolds stress. For the law of the wall and turbulence intensities, the friction velocity given by method 2 was adopted. These procedures were applied without distinction of the flow type despite the fact that the linear shear-stress distribution, the validity of the log law, and the constancy of κ have been questioned in the past for the sediment-laden flows.

Clear-Water Flows

The nondimensional plots for the three clear-water experiments CW01, CW02, and CW03 are shown in Figs. 5 and 6.

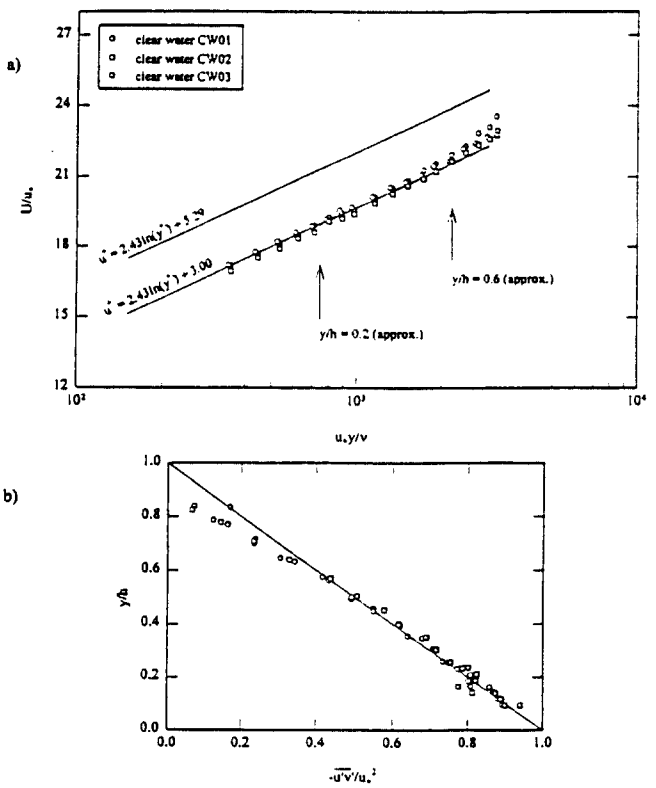

FIG. 5. Mean Profiles for Clear-Water Flows (CW01, CW02, and CW03): (a) Velocity in Wall Coordinates; (b) Reynolds-Shear Stress

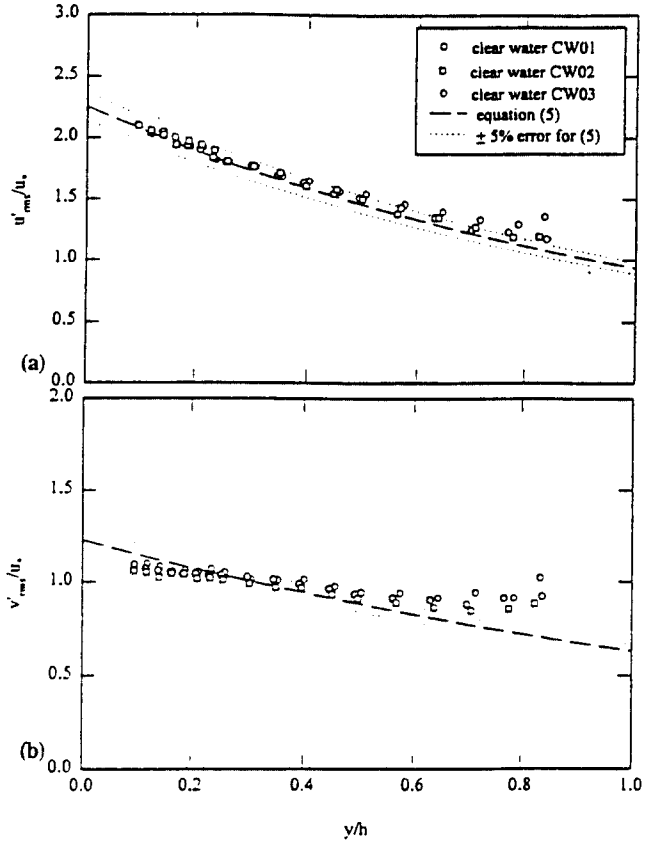

FIG. 6. Turbulence Intensities for Clear-Water Flows (CW01, CW02, and CW03): (a) RMS of Streamwise Velocity Fluctuations; (b) RMS of Vertical Velocity Fluctuations

The good agreement among these data collected over a two-month period indicates good repeatability of flow conditions. From Table 2 it may be observed that a change in the energy slope induced variations of the bulk flow parameters, such as discharge Q, depth h, aspect ratio b/h, bulk velocity U_m, hydraulic radius R, Reynolds number R, and Froude number F, which did not exceed 3.5%. Hence, it may be concluded that, within the limits of experimental uncertainties, the clear-water flows measured under similar conditions.

The increase in the friction velocity with the energy slope is apparent from all methods for its determination. The slight deviation from this trend in the friction velocity for the CW02 experiment, as determined from the Reynolds stress measurements, is an indication that small changes of the traverse position or optical alignment may be involved. This experiment was conducted more than two months after the others. However, this deviation does not contradict the overall conclusions that are drawn later. Ideally, the friction velocities determined by all methods should coincide but there are differences, up to 6%, among methods 1, 2, and 4, an indication of measurement or analysis bias. This level of agreement between the values measured using these three methods also indicates the possible effects of secondary currents in the centerplane of the flume, since these methods implicitly assume two dimensionality of the flow. In contrast, results of method 3 deviate from those estimated using the other methods and are most likely connected to the lack of correction for roughness nonuniformity on the wetted perimeter.

As the channel bottom was rough (concrete), it was necessary to determine the roughness regime of the basic clear-water flow. Using alternative approaches for this determination (Nezu and Rodi 1986; Schlichting 1979; Henderson 1966) and the observed shift in the logarithmic law in Fig. 5(a), it was found that the clear-water flows correspond to the transitional-roughness regime. For reference this also contains the profile for the smooth regime ($B = 5.29$).

The profiles of the mean streamwise velocity U and the Reynolds shear stress ($-\overline{u'v'}$) are plotted in usual wall coordinates in Fig. 5. From Fig. 5(a), the following features are evident: (1) there is good agreement among the data in the logarithmic region; (2) as already noted, the three clear-water flows fall in the transitional-roughness regime and are practically identical in this regard; (3) the velocities in the outer region of the flow ($y/h > 0.6$) deviate systematically from the logarithmic law suggesting the presence of the wake component or/and the effect of the waves on the free surface combined with any free-surface related effects. The Reynolds-stress profiles of Fig. 5(b) show typical data scatter. The linear variation may be taken as evidence of fully developed flow.

The streamwise and vertical (RMS) turbulence intensities, normalized with the friction velocity, are plotted in Fig. 6. On the same plots, empirical correlations proposed by Nezu and Rodi (1986), that is

$$u'_{i\text{RMS}}/u_* = D_i \exp(-C_i\eta) \tag{5}$$

and lines assuming an error interval of ±5% are also presented. The empirical constants used for the plots are: $C_u = 0.88$; $C_v = 0.67$; $D_u = 2.26$; and $D_v = 1.23$. While the agreement (within the experimental scatter) for both streamwise and vertical turbulence intensities is good over much of the channel depth, significant deviations (without increase in scatter) are observed in the upper region of the flow. Nezu and Rodi (1986) pointed out that small waves at the free surface may be responsible for deviations of the streamwise RMS velocity fluctuations of this kind. This conclusion is further supported by the even more noticeable deviations of the vertical fluctuations in the same region, which is contrary to the usual assumption of the damping of these fluctuations near the free surface. More convincing arguments to explain these deviations are given by previous measurements (Parthasarathy and Muste 1994) in the same channel at a lower Froude number (0.21) with much smaller free-surface waves, where the free-surface effect was found to be dominant and the damping of vertical turbulent fluctuations was clearly observed.

Sediment-Laden Flows

By comparing the liquid and particle velocities for the sediment-laden flows SL01, SL02, and SL03, taking each of them as reference flow for the next, the effect of increasing sand concentration could be inferred. The general features mentioned in the previous section for clear-water flows are also valid for these flows: excepting the slopes, all bulk parameters are little changed. A more notable feature seems to be the consistent increase in the friction velocity (3% on average, irrespective of the method of determination) with an increase in sand concentration. It should be noted that, in light of the concept of "equivalent" flows (flows with the same energy slope), the differences in the energy slopes for the pairs CW01-SL01, CW02-SL02, and CW03-SL03 were 0.1%, 0.4%, and 1.7%, respectively.

The mean velocity and Reynolds-stress profiles for the underlying liquid fraction of the sediment-laden flows along with the results for the initial clear-water flow CW01 (the usual way in which comparisons are made in the literature) are shown in Fig. 7. From the velocity profiles of Fig. 7(a), it can be observed that: (1) the data collapse well for all three flows with sediment; (2) the sand addition shifts the logarithmic profiles downward by an average of $\Delta U/u_* \cong 2.3$ units on the u^+ axis; (3) with respect to slope or shape of the profiles, no new feature can be observed. Therefore, it can be noted that the sand addition, by changing flow conditions in the near-bed region,

acts in a way similar to an increase in bed roughness. A similar feature was documented by Wiberg and Rubin (1989), who stated that moving sediment may have an effect an order of magnitude larger than the stationary grain roughness. However, the variation of the velocity shift with sand concentration is not as significant as that found in other studies [for instance, Coleman (1981); Lyn (1986)]. This can be attributed to the rather low sediment concentrations employed in the present experiments and also to the fact that sediment addition did not result in any change in bed roughness. Very large changes in bed roughness are required to produce significant shifts of the logarithmic profiles [see Schlichting (1979) p. 721]. Thus, it would appear that previous results in which such changes were observed might have induced bed-roughness effects (due to sediment deposition). Differences in methods of data analysis, in addition to experimental uncertainties, also might be involved in these differences. From Fig. 7(b) it is observed that the Reynolds-stress profiles for the sediment-laden flows with different concentrations practically coincide on a linear plot indicating that fully developed conditions were satisfied in all cases.

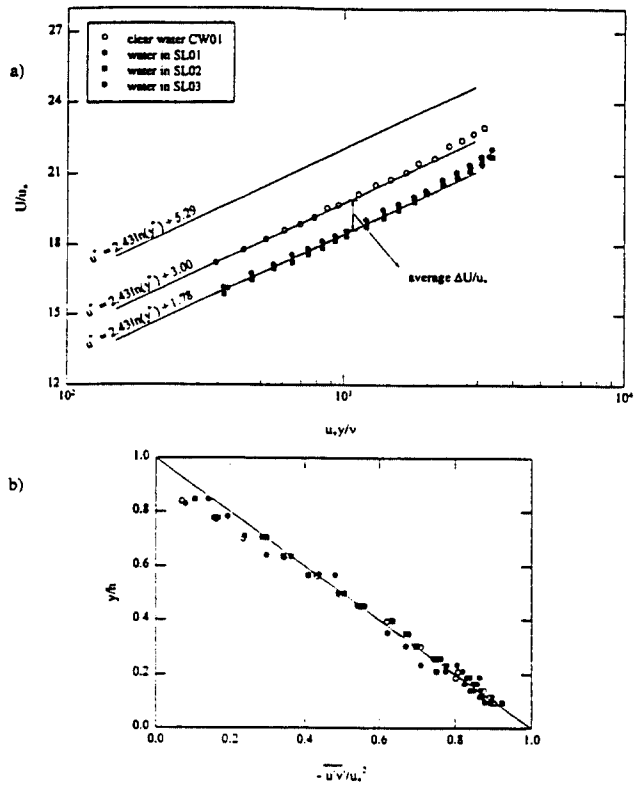

FIG. 7. Mean Profiles for Water in Sediment-Laden Flows (SL01, SL02, and SL03): (a) Velocity in Wall Coordinates; (b) Reynolds-Shear Stress

The relation between the mean streamwise velocity profiles for both phases of the sediment-laden flow, namely underlying water flow and suspended sediment particles, is emphasized in Fig. 8. Velocity profiles for each of the three flows (SL01, SL02, SL03) are plotted separately (shifted downward by 9 units in an expanded view of the logarithmic plot). The corresponding slope-equivalent clear-water flows (CW01, CW02, CW03) are also plotted for reference. Note that the particle velocity profiles are scaled with the friction velocity determined from the water velocity measurements in the corresponding sediment-laden flow. It is clear that, in all cases, the particle velocities are lower than that of the water although there is no consistent trend with concentration. However, the large differences of the highest concentration may be indicative of the liquid-particle interactions. The fact that the particle velocity profile follows a logarithmic relation using the friction velocity determined from the water velocity may seem surprising at first, but this may be the result of the fact that the

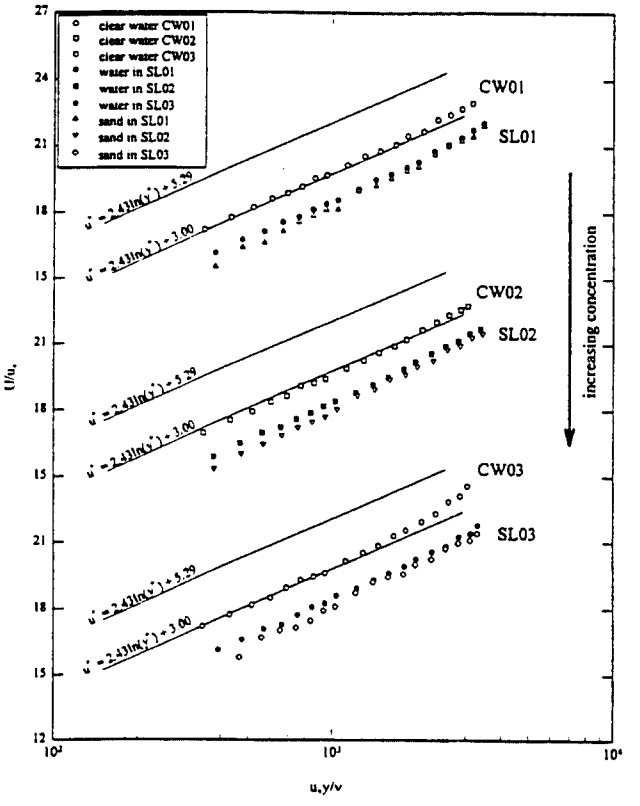

FIG. 8. Velocity Profiles in Wall Coordinates for CW01, CW02, CW03, SL01, SL02, and SL03

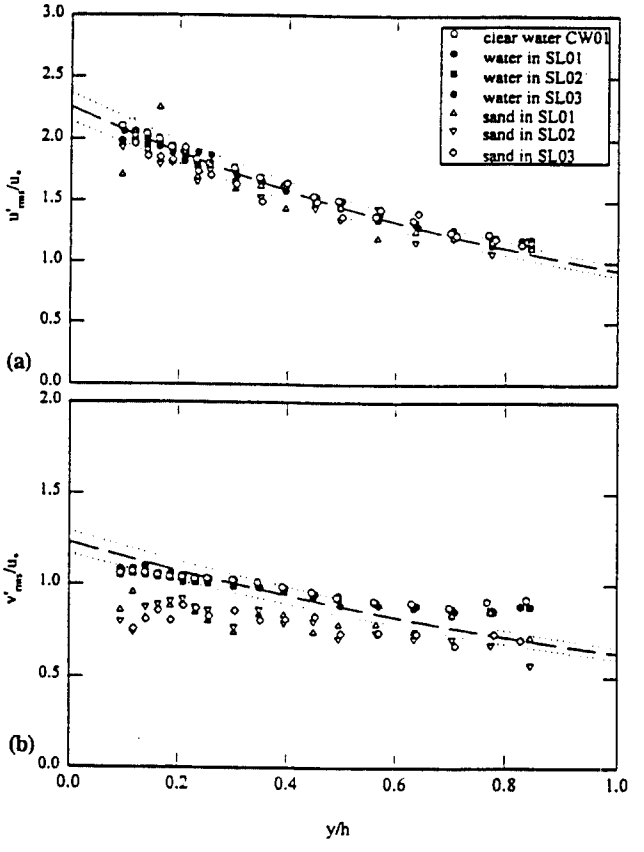

FIG. 9. Turbulence Intensities for Water and Sand in SL01, SL02, and SL03 Flows: (a) RMS of Streamwise Velocity Fluctuations; (b) RMS of Vertical Velocity Fluctuations

wall shear stress remains the variable that controls the flow in the near-wall region.

Fig. 9 shows profiles of the turbulence intensities of both the liquid and sand particles. The turbulence intensities for the initial clear-water flow (CW01), which is representative of the CW02 and CW03 flows, are also plotted. While the liquid turbulence intensity distribution do not show any distinct feature when compared to the initial clear-water flow or to the Nezu and Rodi (1986) correlation, a significant difference can be noted for the particle velocity fluctuations. A slight decrease in the streamwise particle velocity fluctuations is observed in Fig. 9(a), and a very significant decrease and even change in shape for the vertical velocity fluctuations is seen in Fig. 9(b). The trends in both quantities are consistent throughout the depth and for different sediment concentrations. Recall that the liquid information is based on a much larger sample than that for particles. The influence of the sample size is, in fact, evident from the increased scatter of the particle turbulence intensities. In spite of the scatter, the decrease in the particle velocity fluctuations, and particularly that of the vertical fluctuations, is unmistakable. However, a plausible explanation of these trends is not yet available.

SUMMARY AND CONCLUSIONS

Using the newly developed DLDV technique experiments were performed to obtain velocity measurements in open-channel flows with and without suspended sediment. The data were analyzed for both mean velocity and turbulence characteristics of the liquid and sediment particles. The measurements and their analysis showed that some generally accepted assumptions regarding the liquid and sediment phases in sediment-laden flows need to be reevaluated. With the narrow range of experimental conditions of the present work in mind, the most important findings and consequent implications are as follows.

There exists a slip (velocity difference) between the liquid and sediment; the streamwise velocity of sediment in these open-channel experiments with 0.21–0.25 mm sand in suspended transport was less than that of water by as much as 4%. The existence of slip between the sediment and liquid was presumed in previous work [see Bagnold (1973); Lazendorf (1985); Schoellhamer (1986)], but its quantification was found to be difficult.

In spite of the limited range of sediment concentrations employed, the present study revealed that the mean velocity, when compared to an equivalent flow, shows a continuous decrease with sediment concentration throughout the depth of flow. Such effects are expected to be higher in flows with larger concentrations.

Based on intuitive arguments rather than clear experimental evidence, it has been generally accepted that turbulence is damped in the presence of sediment. The present measurements show that the particle velocity fluctuations were smaller than for the liquid without a discernible influence on the liquid turbulence characteristics. However, this may be dependent on the hydraulic conditions, and more work is required to determine specific features of turbulence structure in sediment-laden flows.

Given the fact that only small changes in flow parameters follow sediment addition, the need for more accurate instrumentation and experimental designs (detailed operating and environmental conditions) for investigation of sediment-laden flows becomes clear.

The present results show that further studies are required for extended range of the sediment size, concentration, and flow conditions. If the present findings are confirmed over a wide range of parameters, previous experimental data and theoretical models may have to be revised to include the difference between particle and liquid velocities. Given the increased complexity of such an approach and the lack of understanding of the basic flow process it is expected that experiments will still remain the main tool of investigation in sediment-laden flows.

ACKNOWLEDGMENTS

Initial support of this research was provided by the National Science Foundation under grant CTS-9021149. The study was completed with financial support from the Iowa Institute of Hydraulic Research. The writers thank R. N. Parthasarathy for many helpful discussions regarding the DLDV system and for reviewing an early draft of this paper.

APPENDIX I. REFERENCES

Aziz, N. M. (1996). "Error estimate in Einstein's suspended sediment load method." *J. Hydr. Engrg.*, ASCE, 122(5), 282–285.

Bagnold, R. A. (1973). "The nature of saltation and of 'bed-load' transport in water." *Proc., Royal Soc. of London*, London, England, A332, 473–504.

Coleman, N. L. (1981). "Velocity profiles with suspended sediment." *J. Hydr. Res.*, IAHR, Delft, The Netherlands, 19(3), 211–227.

Durst, F., Melling, A., and Whitelaw, J. H. (1981). *Principles and practice of laser-Doppler anemometry*, 2nd Ed., Academic Press, Inc., San Diego, Calif.

Henderson, F. M. (1966). *Open channel flow*. Macmillan Inc., Greenwich, Conn.

Hoyt, J. W. (1991). "'Negative Roughness' and Polymer Drag Reduction," *Experiments in Fluids*, 11(2/3), 142–146.

Jobson, H. E., and Sayre, W. W. (1970). "Vertical transfer in open channel flow." *J. Hydr. Div.*, ASCE, 96(10), 703–724.

Kereselidze, N. B., and Kutavaia, V. I. (1995). "Experimental research on kinematics of flows with high suspended solid concentration." *J. Hydr. Res.*, IAHR, Delft, The Netherlands, 33(1), 65–76.

Lazendorf, W. (1985). "On the motion of solids in viscous sublayers of a pipe flow." *Proc., Euromech 192: Transport of Suspended Solids in Open Channel*, 43–46.

Lyn, D. A. (1986). "Turbulence and turbulent transport in sediment-laden open-channel flows." *Rep. No. KH-R-49*, W. M. Keck Laboratory, California Inst. of Technol., Pasadena, Calif.

Lyn, D. A. (1988). "A similarity approach to turbulent sediment-laden flows in open channels." *J. Fluid Mech.*, 193, 1–26.

Müller, A. (1973). "Turbulence measurements over a movable bed with sediment transport by laser-anemometry." *Proc., 15th Congr., IAHR*, 43–50.

Muste, M. (1995). "Particle and liquid velocity measurements in sediment-laden flows with a discriminator laser-Doppler velocimeter," PhD thesis, Univ. of Iowa, Iowa City, Iowa.

Muste, M., Parthasarathy, R. N., and Patel, V. C. (1996). "Discriminator laser-Doppler velocimetry for measurement of liquid and particle velocities in sediment-laden flows." *Experiments in Fluids*, 22, 45–56.

Nezu, I., and Rodi, W. (1986). "Open-channel flow measurements with a laser-Doppler anemometer." *J. Hydr. Engrg.*, ASCE, 112(5), 335–355.

Parker, G., and Wilcock, P. R. (1993). "Sediment feed and recirculating flumes: fundamental difference." *J. Hydr. Engrg.*, ASCE, 119(11), 1192–1204.

Parthasarathy, R. N. (1989). "Homogeneous dilute turbulent particle-laden water flows," PhD thesis, Univ. Michigan, Ann Arbor, Mich.

Parthasarathy, R. N., and Muste, M. (1994). "Velocity measurements in asymmetric turbulent channel flows." *J. Hydr. Engrg.*, ASCE, 120(9), 1000–1020.

Prinos, P., and Zeris, A. (1995). "Uniform flow in open-channels with movable gravel bed." *J. Hydr. Res.*, IAHR, Delft, The Netherlands, 33(5), 705–719.

Rashidi, M., Hetsroni, G., and Banerjee, S. (1990). "Particle-turbulence interaction in a boundary layer." *Int. J. Multiphase Flow*, 16(6), 935–949.

Rogers, C. B., and Eaton, J. K. (1989). "The interaction between dispersed particles and fluid turbulence in a flat plate turbulent boundary layer in air." *Rep. MD-52*, Stanford Univ., Calif.

Schlichting, H. (1979). *Boundary-layer theory*, 7th Ed., McGraw-Hill, New York, N.Y.

Schoellhamer, D. H. (1986). "Comparison of mean longitudinal suspended-sediment and stream velocities." *Proc., 3rd Int. Symp. on River Sedimentation*, Univ. Mississippi, University, Miss., 814–823.

Song, T., Graf, W. H., and Lemmin, U. (1994). "Uniform flow in open channels with movable gravel bed." *J. Hydr. Res.*, IAHR, Delft, The Netherlands, 32(6), 861–876.

Summer, B. M., and Deigaard, R. (1981). "Particle motions near the bottom in turbulent flow in an open channel." Part 2, *J. Fluid Mech.*, 109, 311–337.
Tsuji, Y., and Morikawa, Y. (1982). "LDV measurement of an air-solid two-phase flow in an horizontal pipe." *J. Fluid Mech.*, 120, 385–409.
Valiani, A. (1991). "The von-Karman coefficient in sediment-laden flow." *J. Hydr. Res.*, IAHR, Delft, The Netherlands, 29(1), 129–136.
Van Ingen, C. (1981). "Observations in a sediment-laden flow by use of laser-Doppler velocimetry." *Rep. KH-R-42*, W. M. Keck Lab., California Inst. of Technol., Pasadena, Calif.
Vanoni, V. A. (1975). "Suspension of sediment." *Sedimentation Engrg.*, V. A. Vanoni, ed., ASCE, New York, N.Y.
Wang, G. Q., and Ni, J. R. (1991). "The kinetic theory for dilute solid/liquid two-phase flow." *Int. J. Multiphase Flow*, 17(2), 273–281.
Wang, Z., and Larsen, P. (1994). "Turbulent structure of water and clay suspensions with bed load." *J. Hydr. Engrg.*, ASCE, 120(5), 577–600.
Wang, X., and Qian, N. (1992). "Velocity profiles of sediment-laden flow." *Int. J. Sediment Res.*, IRTCES, Beijing, China, 7(1), 27–58.
Wiberg, P. L., and Rubin, D. M. (1989). "Bed roughness produced by saltating sediment." *J. Geophysical Res.*, 94(C4), 5011–5016.
Yalin, M. S. (1977). *Mechanics of sediment transport*. Pergamon Press, New York, N.Y.

APPENDIX II. NOTATION

The following symbols are used in this paper:

B = additive constant in logarithmic law for smooth walls;
b = width of channel;
D = sediment diameter;
D_{50} = median particle diameter;
F = Froude number;
g = acceleration due to gravity;
h = depth of flow;
Q = discharge;
R = hydraulic radius;
R = Reynolds number based on mean velocity;
S = free-surface (energy) slope;
S_b = bed slope for the channel;
U = mean horizontal velocity;
U_m = mean bulk velocity;
u = instantaneous horizontal velocity; $u = U + u'$;
u' = horizontal fluctuating velocity;
u^+ = mean streamwise velocity normalized with u_*;
u_* = friction velocity (bed shear velocity);
$u'_{\mathrm{RMS}} = \sqrt{\overline{u'^2}}$ = root mean square of horizontal fluctuating velocity;
v' = vertical fluctuating velocity;
$v'_{\mathrm{RMS}} = \sqrt{\overline{v'^2}}$ = root mean square of vertical fluctuating velocity;
y = distance from bed surface;
y^+ = distance from bed normalized with wall variables;
η = nondimensional flow depth;
κ = von Karman coefficient;
ν = kinematic viscosity;
τ = total shear stress (molecular and turbulent); and
τ_b = bed shear stress.